

Analytical Methods

Accepted Manuscript



This is an *Accepted Manuscript*, which has been through the Royal Society of Chemistry peer review process and has been accepted for publication.

Accepted Manuscripts are published online shortly after acceptance, before technical editing, formatting and proof reading. Using this free service, authors can make their results available to the community, in citable form, before we publish the edited article. We will replace this *Accepted Manuscript* with the edited and formatted *Advance Article* as soon as it is available.

You can find more information about *Accepted Manuscripts* in the [Information for Authors](#).

Please note that technical editing may introduce minor changes to the text and/or graphics, which may alter content. The journal's standard [Terms & Conditions](#) and the [Ethical guidelines](#) still apply. In no event shall the Royal Society of Chemistry be held responsible for any errors or omissions in this *Accepted Manuscript* or any consequences arising from the use of any information it contains.

1
2
3
4
5
6
7
8
9
10
11
12
13
14
15
16
17
18
19
20
21
22
23
24
25
26
27
28
29
30
31
32
33
34
35
36
37
38
39
40
41
42
43
44
45
46
47
48
49
50
51
52
53
54
55
56
57
58
59
60

Multiway calibration coupling with fluorescence spectroscopy to determine magnolol and honokiol in herb and plasma samples

Leqian Hu *, Chunling Yin

School of Chemistry and Chemical Engineering, Henan University of Technology, Zhengzhou 450001, China

*Corresponding author. Fax: +86-371-67756718

E-mail address: leqianhu@163.com

Abstract

This work presented a novel approach for simultaneous determination of mixtures of magnolol and honokiol in herb and plasma samples by combining the sensitivity of molecular fluorescence and the selectivity of the second-order calibration method. The excitation-emission fluorescence matrix data was processed by applying the second-order calibration method based on the parallel factor analysis (PARAFAC) and self-weighted alternating trilinear decomposition (SWATLD) algorithms. The results showed that the method could solve the problem of analysis of complex multi-components, with “mathematics separation” to replace some or enhance chemical separation. The recoveries from spiked herb samples were in the ranges 93-104% for magnolol and 89-98% for honokiol, and from spiked human plasma samples were in the ranges 98-105% for magnolol and 94-96% for honokiol. In herb samples, the LOD of magnolol was 0.51 $\mu\text{g/ml}$ and 0.45 $\mu\text{g/ml}$, and 0.37 $\mu\text{g/ml}$ and 0.24 $\mu\text{g/ml}$ for honokiol by PARAFAC and SWATLD. For human plasma samples, the LOD of magnolol was 0.93 $\mu\text{g/ml}$ and 0.64 $\mu\text{g/ml}$, and 0.79 $\mu\text{g/ml}$ and 0.42 $\mu\text{g/ml}$ for honokiol, respectively. The results demonstrated that this method had both high recovery and good precision for honokiol and magnolol. The proposed method avoided preconcentration and with only simple disposal process, so it considerably decreased the analytical time and the experimental expenses. Thus it can be considered as a green analytical procedure for magnolol and honokiol determination in herb and plasma samples.

Keywords Magnolol; Honokiol; Excitation-emission fluorescence; Parallel factor analysis; Self-weighted alternating trilinear decomposition

Introduction

Nowadays, with the requirement of more therapeutic efficacy and less adverse effects, a renewed interest has been generated in herb medicines of traditional Chinese medicine. Magnolol and honokiol are polyphenolic compounds derived from Cortex *Magnolia officinalis*, a plant commonly in many traditional Chinese medicine (TCM) prescriptions [1]. It was discovered that magnolol and honokiol could inhibit hydroxyl radicals and lipid peroxidation as early as 1990 [2]. Now abundant study showed they also possess anti-oxidative, anti-inflammatory, anti-tumorigenic, anti-diabetic, anti-anxiety, anti-microbial, anti-neurodegenerative and anti-depressant properties [3-9]. They were also to be proven to reduce allergic and asthmatic reactions. Research demonstrated that they might have therapeutic potential for the treatment of thrombotic stroke [10], typhoid fever, headache, stomach inflammations [11], depression and acute neurodegenerative diseases [12]. Some concentrated composite herbal preparations that contain Cortex *Magnoliae Officinalis* in their prescriptions, such as Xiangsha yangwei pills, Ping-wei tablet, Muxiang shunqi pills (both to be used to treat stomach diseases) and Niantong pills (to treat typhoid fever) are widely used in oriental countries for their convenient use. Magnolol and honokiol are the major pharmacologically active components in these Chinese patent medicines.

In view of many in-progress researches associated with magnolol and honokiol, some rapid, efficient, sensitive and accurate approaches analytical methods are required to facilitate these studies. In the same time, with a view to the safety considerations and the quality control of herbal medicine, determination of the total content of major pharmacologically active components is also an important parameter for evaluating the quality of herb. Such as, the Department of Health in Taiwan requested that all concentrated herbal preparations submitted for registration should include the determination of at least two chemical constituents as markers after 1995 [13]. The Pharmacopoeia of China required the total content of honokiol and magnolol in Cortex *Magnoliae Officinalis* to be no less than 2.0% [14]. Further, in order to promote the Good Manufacture Practice (GMP) of Chinese medicinal preparations, determination the concentrations of magnolol and honokiol are also necessary from pharmacokinetics perspective.

1
2
3
4
5
6
7
8
9
10
11
12
13
14
15
16
17
18
19
20
21
22
23
24
25
26
27
28
29
30
31
32
33
34
35
36
37
38
39
40
41
42
43
44
45
46
47
48
49
50
51
52
53
54
55
56
57
58
59
60

Some analytical methods have been reported to quantitatively determine the magnolol and honokiol in different samples. The most frequently used method for the determination of honokiol and magnolol was high-performance liquid chromatography (HPLC), including ion-pair high-performance liquid chromatography [13,15-16], supercritical fluid chromatography [17], high speed counter current chromatography [18] and liquid column chromatography-mass spectrometry [19], etc. Capillary electrophoresis (CE) had also been applied in the analysis of magnolol and honokiol in *Magnolia officinalis* [14, 20-21]. However, only a few studies have been described for the simultaneous determination of honokiol and magnolol by spectroscopy technology [22,23]. The reason maybe because they are isomers to each other and the spectra of them is always serious overlapping. They can not be determined simultaneously by spectrophotometry without the help of chromatography separation or similar methods.

The aim of our work is to develop and validate a novel fluorometry method for simultaneous quantification magnolol and honokiol in herb and plasma samples. Fluorescence spectroscopy is an attractive alternative to chromatographic methods. Unfortunately, the application of fluorescence techniques for pharmaceutical analysis has been limited by the lack of selectivity of fluorescence spectroscopy. The broad character of both the excitation and emission fluorescence bands curtails the possibility of finding a unique excitation and emission wavelength for each potential analyte. The development of multi-way calibration techniques, especially second-order calibration methods, may bridge the gap by mathematically decomposing the overlapping profile into the pure profiles of each chemical species even the unknown interference [24]. This property is called “second-order advantage” [25-27]. This fact means that collection of entire excitation-emission matrix (EEM) fluorescence spectra followed by application of advanced multi-way spectral deconvolution and calibration algorithms overcomes the limitations of fluorescence spectroscopy, yet achieving accurate quantification of the analytes of interest in complex matrices. The use of second-order calibration to resolve overlapping spectra of target analyte has been demonstrated in many areas of research [26, 28]. It allows one to save time and money, and reduce the use of harmful chemical solvents. So, our interest is to utilize excitation-emission fluorescence combining with multi-way calibration to facilitate the quantitative analysis of magnolol and honokiol in the

complex mixture.

2. Theory

2.1. Trilinear model for second-order resolution

The mathematical formulation of excitation-emission fluorescence spectroscopy for N components samples can also be expressed as the following

$$x_{ijk} = \sum_{n=1}^N a_{in} b_{jn} c_{kn} + e_{ijk} \quad (1)$$

$$(i = 1, \dots, I; j = 1, \dots, J; k = 1, \dots, K)$$

Where x_{ijk} is the intensity of the k th sample at i th excitation wavelength and at j th emission wavelength. N is the total number of detectable components (i.e. number of factors or chemical rank). a_{in} , b_{jn} and c_{kn} are the elements of the loading matrices **A**, **B** and **C**, respectively. **A** and **B** are the emission spectral and excitation spectral profiles matrices for all N components, respectively. **C** denotes the relative concentration matrix. These can be expressed as $\mathbf{A} = (\mathbf{a}_1, \mathbf{a}_2, \dots, \mathbf{a}_n)$, $\mathbf{B} = (\mathbf{b}_1, \mathbf{b}_2, \dots, \mathbf{b}_n)$ and $\mathbf{C} = (\mathbf{c}_1, \mathbf{c}_2, \dots, \mathbf{c}_n)$. e_{ijk} is the element of the measurement error matrix which contains the variation not captured by the model.

In contrast with bilinearity, the above equation can be considered to being trilinearity. It can be viewed as an extension of Beer's law to second-order data [25]. This amounts to assuming that the measured peak is the sum of the individual peaks of each analyte and that the emission spectral and excitation spectrum of one analyte are proportional in all the samples. The main reason for this continuing interest is that second-order and higher-order data are able to deal with potential interferences in real samples. In contrast to both zero-order and first-order calibrations, potential interferences not included in the calibration set can be modeled. Second calibration allows us to quantify accurately the calibrated analytes even in the presence of unknown constituents. The chemometric literature has coined the expression "second-order advantage" to describe the latter property [25]. As a consequence, the decomposition of a three-way data array built with response matrices measured for a number of samples is often unique, allowing emission spectral profile and excitation spectral profiles, as well as relative concentrations of individual sample components to be extracted directly.

Numbers of second-order calibration methods used to resolve multicomponent

1
2
3
4
5
6
7
8
9
10
11
12
13
14
15
16
17
18
19
20
21
22
23
24
25
26
27
28
29
30
31
32
33
34
35
36
37
38
39
40
41
42
43
44
45
46
47
48
49
50
51
52
53
54
55
56
57
58
59
60

mixtures have been proposed. They included the generalized rank annihilation method (GRAM) [29], parallel factor analysis (PARAFAC) [30], alternating trilinear decomposition (ATLD) [31], coupled vectors resolution (COVER) [32], self-weighted alternating trilinear decomposition (SWATLD) [33], multivariate curve resolution coupled to alternating least squares (MCR-ALS) [34], etc. In the second-order calibration algorithms, the PARAFAC and SWATLD methods were proved to be very useful for the three-way data measured from the fluorophotometer [35].

2.2. PARAFAC

PARAFAC is a generalization of principal component analysis (PCA) to higher orders. The algorithm used to solve the PARAFAC model is alternating least squares (ALS) [26]. One can obtain A, B and C from the following equation by alternating least squares principle.

$$F(\mathbf{A}, \mathbf{B}, \mathbf{C}) = \sum_{k=1}^K \left\| \mathbf{X}_{\cdot k} - \mathbf{A} \mathbf{diag}(\mathbf{c}_k^T) \mathbf{B}^T \right\|_F^2 \quad (2)$$

ALS successively assumes the loadings in two modes and then estimates the unknown set of parameters of the last mode. The algorithm converges iteratively until the relative change in fitting between two iterations is below a certain value (the default is 10^{-6}). It is initialized by either random values or values calculated by a direct trilinear decomposition based on the generalized eigenvalue problem. Constraining the PARAFAC solution can sometimes be helpful in terms of the interpretability or the stability of the model. The resolution of spectra used to require the non-negativity constraint since negative spectral parameters do not make sense.

2.3. SWATLD

The PARAFAC algorithm is based on a least-squares minimization, whereas SWATLD uses a procedure known as alternating trilinear decomposition [33]. The underlying theories have been recently reviewed [28]. Comparing with the PARAFAC algorithm, One can obtain A, B and C from the following equations by alternating least squares principle.

$$F(\mathbf{A}) = \left\| \mathbf{X}_{I \times JK} - \mathbf{A}(\mathbf{B} | \otimes | \mathbf{C})^T \right\|_F^2 \quad (3)$$

$$F(\mathbf{B}) = \left\| \mathbf{X}_{J \times IK} - \mathbf{B}(\mathbf{A} | \otimes | \mathbf{C})^T \right\|_F^2 \quad (4)$$

$$F(\mathbf{C}) = \sum_{k=1}^K \left\| \mathbf{X}_{I \times JK} - \mathbf{A} \mathbf{diag}(\mathbf{c}_k^T) \mathbf{B}^T \right\|_F^2 \quad (5)$$

1
2
3
4
5
6
7
8
9
10
11
12
13
14
15
16
17
18
19
20
21
22
23
24
25
26
27
28
29
30
31
32
33
34
35
36
37
38
39
40
41
42
43
44
45
46
47
48
49
50
51
52
53
54
55
56
57
58
59
60

Comparing the PARAFAC algorithm, the SWATLD algorithm has the advantages of fast convergence and insensitivity to the excess factors used in calculations. According to some experience, it offers better results than other second-order algorithms. There is a more detailed explanation of the algorithm in the cited reference [33].

All computer programs were written in the MATLAB (MathWorks) programming environment, and all calculations were carried out on a Windows 7 operating system.

3. Experimental

3.1. Reagents and solutions

Magnolol and honokiol were purchased from National Institute for the Control of Pharmaceutical and Biological Products (Beijing, China). Cortex Magnoliae Officinalis and Ping-wei tablet were obtained from Tong-Ren-Tang Traditional Chinese Medicine Store (BeiJing, China).

All aqueous solutions were made up in doubly distilled water. Other chemicals were of analytical grade. Stock solutions of magnolol (8.760mg/ml) and honokiol (7.200mg/ml) were separately prepared in sodium hydroxide and were kept in a 4°C refrigerator. The stock solutions were diluted with acetic acid/sodium acetate buffer solution (pH = 3) to the desired concentration just prior to use.

3.2 Sample preparation

Ping-wei tablet is a herbal prescription often used for treating patients with abdominal fullness and distention, nausea and vomiting, belching, chronic gastritis and duodenal ulcer. It is composed of rhizoma atractylodis, glycyrrhiza, pericarpium citri reticulatae and Magnoliae Cortex etc. A 1.0030 g sample of Ping-wei tablet was extracted with 95% methanol (40ml) by ultrasound with 3500 rpm at room temperature for 10 min and left for 24 h, then continuing ultrasound at 500 rpm for 10 min. The supernatant was filtered through a No.1 filter-paper to a volumetric flask. The residue was washed three times and filtered to the volumetric flask. At last the herbal preparation extract was diluted to 100 ml with 95% methanol.

Magnoliae Cortex was first dried at 60°C for 2 h and then was pulverized. A 1.0827 g powder was weighed accurately and dispersed in 40ml of methanol. The mixture was kept in a 60°C water bath for 3 h. After cooling, it was sonicated for 30min and filtered through a filter paper. The extract was diluted to 100 ml with 95%

methanol.

3.3 Plasma sample

Plasma received from the center of blood in ZhengZhou obtained from healthy volunteers was used to prepare the predicted samples. Treatment of plasma samples was according to the published method [14]. Different content of magnolol and honokiol were spiked to the 2ml plasma sample separately then centrifuged at 3000 rpm for 10 min. The resulting plasma sample was then vortex-mixed with acetonitrile. After 15 min, the mixture was centrifuged at 3000 rpm for 5 min to remove proteins. The supernatant was then separately transferred into a 10 ml tube containing 50–60 mg sodium chloride. The suspension was vortex-mixed briefly and incubated at room temperature for 20 min and was vortex-mixed again. Finally, the plasma sample was centrifuged at 3000 rpm for 5 min. The supernatant was diluted to 10ml in buffered solution and subjected to fluorometric analysis.

3.4 Calibration and Prediction samples

A calibration set of 10 samples (C01–C10) was constructed. They only contained magnolol and honokiol. The concentrations of magnolol and honokiol were randomly selected, covering the linear range of concentrations and avoiding the collinearity between analytes. All the analyte concentrations of calibration samples were listed in Table 1. In these samples, no interferences were added.

Table 1. Concentrations of magnolol and honokiol in calibration samples.

calibration sample	Added concentration($\mu\text{g}/\text{ml}$)	
	magnolol	honokiol
C01	0	108.0
C02	140.1	0
C03	131.4	86.42
C04	157.7	72.00
C05	175.2	57.63
C06	70.08	86.41
C07	87.60	72.00
C08	105.1	93.62
C09	122.6	79.21
C10	140.2	57.60

A prediction set of 12 samples was constructed. In these samples, four samples were Magnoliae Cortex samples, PM0 was only the extract of Magnoliae Cortex (2 ml), and PM1-PM3 were spiked with suitable amounts of standard magnolol and honokiol solutions besides the 2ml extract of Magnoliae Cortex (treated as explained

in Section 3.2). The other four samples were Ping-wei tablet, PP0 was only the 2 ml extract of Ping-wei tablet. PP1-PP3 were also spiked with suitable amounts of standard magnolol and honokiol solutions besides the 2 ml extract of Ping-wei tablet. The last four samples were plasma samples. PB0 was only the supernatant of plasma samples, and PB1-PB3 were also spiked with different amounts of standard magnolol and honokiol solutions besides the supernatant of plasma. All the analyte concentrations of prediction samples can be found in Table 2 and Table 3. At last the above samples were all diluted to 10ml in buffered solution to minimize the difference of each sample.

3.5 Apparatus and conditions

The EEMs were measured on a Varian Eclipse fluorescence spectrophotometer in scan mode. In all cases, a 1.00 cm quartz cell was used. To avoid the Rayleigh and Raman scatterings, a collection of emission scans from 295 to 495 nm with 5 nm increments was obtained at varying excitation wavelengths ranging from 210 to 310 nm with 5 nm increment. The bandwidths were all 5 nm for excitation and emission, and the scan rate was 2400 nm/min. Each scan was comprised of 42 emission and 21 excitation wavelengths.

Because a single-measurement EEM fluorometer lacks the baffles and filters typically present in scanning fluorometers, therefore, the intensity of the Rayleigh and Raman scattering is unmitigated. These diagonal patterns across the spectra are inefficiently modeled by trilinear calibration methods. This problem is easily solved by applying the blank spectra. In this trial, background and noise components were all subtracted from the spectra by blank samples.

4. Results and discussion

4.1 Effect of the pH on the fluorescence intensity of magnolol and honokiol.

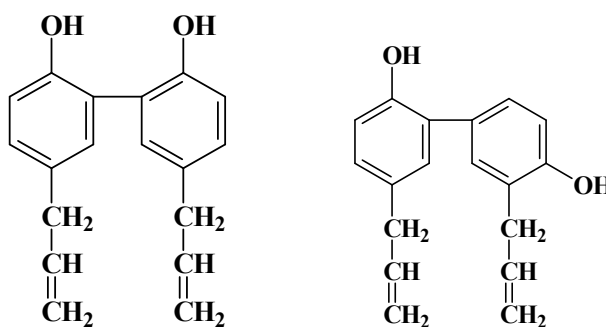


Fig. 1 Molecular structure of magnolol (left) and honokiol (right).

Chemical structures of magnolol and honokiol are shown in Figure 1. Their fluorescence intensity depends on the degree of protonation. In order to enhance the sensitivity and resolution of analytes, the effect of the pH on the fluorescence intensity of magnolol and honokiol was studied in this research. The result was shown in Figure 2. The buffered solutions were acetic acid/sodium acetate buffers at five different pH values (2.0, 3.0, 4.0, 5.0 and 6.0). As shown in Figure 2, the influence of pH for magnolol and honokiol was slightly different. But in general, their fluorescence intensity increased with increasing the pH value and decreased quickly when the pH value exceeded four. The changes of the pH value were due to the dissociation of the hydroxyl groups for both analytes. In this experiment, acetic acid/sodium acetate buffer at pH of 3.0 was chosen as the buffer solution in considering the fluorescence intensity.

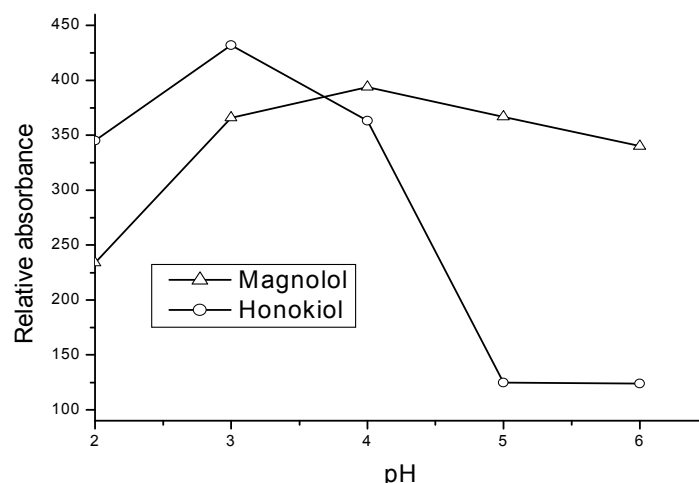


Fig. 2 Effect of the pH on the fluorescence intensity of magnolol and honokiol.

4.2 Effect of the SDS on the fluorescence intensity of the analytes.

The luminescence intensity is often enhanced by the addition of surfactant. In this work, the effects of surfactant (sodium dodecyl sulfonate, SDS) concentrations were also investigated. Five different concentrations of SDS (0.03, 0.05, 0.07, 0.08 and 0.09 mol/L) were added into the same content analytes, respectively. Figure 3 showed the effect of the different concentration of SDS on the fluorescence intensity of the magnolol and honokiol. We could find that the different concentration SDS had small effect to magnolol but a big impact to honokiol. Taking into consideration of various effects, 0.07 mol/L SDS was applied in this research to enhance the sensitivity of the analytes.

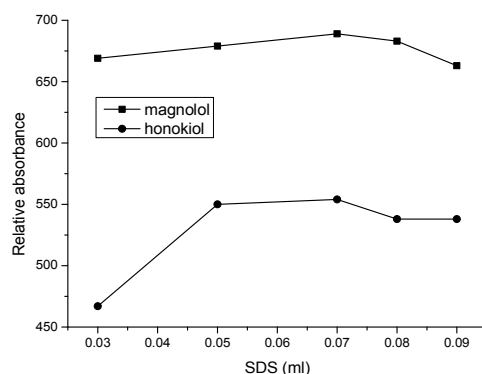


Fig.3 Effect of different concentration SDS on the fluorescence intensity of magnolol and honokiol.

4.3 Number of Factors.

Firstly, the optimum number of factors was calculated. In the case of PARAFAC, the chemical rank is defined as the number of significant factors distinguishing from noise. When using PARAFAC, it requires an accurate estimation of the chemical rank (i.e. the optimum number of factors) in the system studied, and either underestimation or overestimation of the chemical rank often leads to erroneous results. Even for SWATLD, which is insensitive to the overestimation of the chemical rank of a three-way data array, it still requires that the chemical rank chosen is not less than the real one of a three-way data array studied. Therefore, deciding the underlying species in the mixture is always the key step to further qualitative and quantitative analysis, especially for the real analysis system. A number of suitable methods for estimating the chemical rank have been developed in the literature. Bro and Kiers [36] suggested obtaining the number of responsive components (N) by consideration of the internal parameter known as core consistency diagnosis (CORCONDIA), which was a measure of how well a given model was able to reproduce the so called Tucker core of a cube of data. The core consistency was calculated as a function of a trial number of components. It remained near a value of 100 when the number was less than or equal to the optimum, for exceeding component numbers it drops below 50%.

First, the EEM data of Magnoliae Cortex and Ping-wei tablet were researched. Unconstrained PARAFAC models of this EEM data were developed using one to ten components, and the percentage of fitting was used as the initial approach to select the number of factors. Figure 4(a) showed the value obtained for the 18-sample (including 10 calibration samples and 8 prediction samples) cube when studying the Magnoliae

Cortex and Ping-wei tablet sample. As could be seen, the core consistency dropped to a very low value when using four components to model the cube, suggesting that $N = 3$ was a sensible choice. It was more than the true number of spectroscopically absorbing species that were expected based on standard samples. It indicated that the trilinear data arrays requested to be fitted exactly with three factors. It showed that some interferences were introduced to the real mixture system. These interferences were retrieved as a single component by PARAFAC and similar methods.

On the other hand, anyone of these methods cannot ensure to obtain the accurate result for a practical mixture system. Two or more methods are often used to estimate the appropriate component number of the mixture to confirm the result [28]. We also suggested a simple linear transform incorporating Monte Carlo simulation approach (which names LTMC) to determine the component number of the three-way data arrays [37]. Figure 4(b) showed that the number of chemical species presenting in Magnoliae Cortex and Ping-wei tablet, estimated by LTMC. The projection residuals for the former three factors were relatively small but a rapid increasing for the later factors. Because the first three factors represented the real factors spaces, the later factors represented the noise spaces. It also showed that the trilinear datasets requested to be fitted exactly with three factors. This was coincident with the result obtained by CORCONDIA.

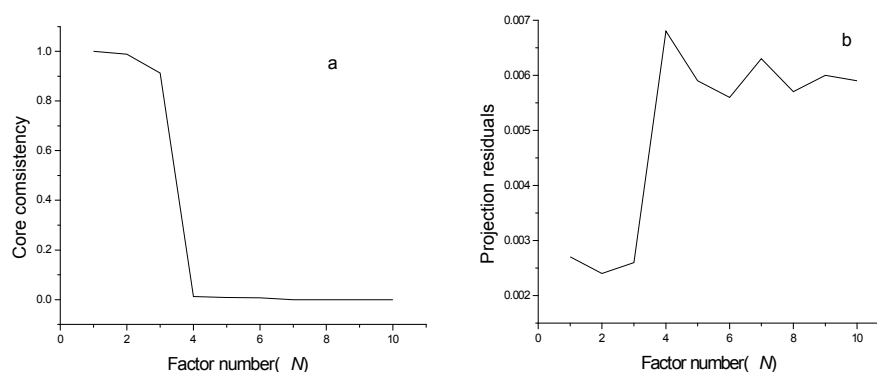


Fig. 4 The results of factor-determining of the EEM data arrays by CORCONDIA (a) and LTMC (b).

The EEMs data of plasma sample was also analyzed by CORCONDIA and LTMC algorithms, separately. Similarly, they all showed that the new trilinear data arrays requested to be fitted exactly with three factors. The figure was not showed due to the same as the front research.

4.5 PARAFAC and SWATLD Analysis.

In Figure 5, the EEMs for pure magnolol and honokiol (A), for Magnoliae Cortex (B), for Ping-wei tablet (C) and for magnolol and honokiol in plasma (D) were plotted. As shown in Figure 5 (A), honokiol presented a broad emission band with a peak value at 350 nm and two excitation maxima at 240 and 280 nm. Likewise, magnolol was found with two excitation maxima at 245 and 280 nm and an emission peaks at 385 nm, respectively.

Due to overlap of the excitation-emission spectra of the analytes from each other and with the constituents of the samples, it is necessary to use second-order calibration to address this situation. In this paper, PARAFAC and SWATLD algorithms were recommended to assay the contents of magnolol and honokiol in complex matrices, which fully exploited the “second order advantage” to accomplish reliable resolution of spectra and accurate quantification of individual components of interest.

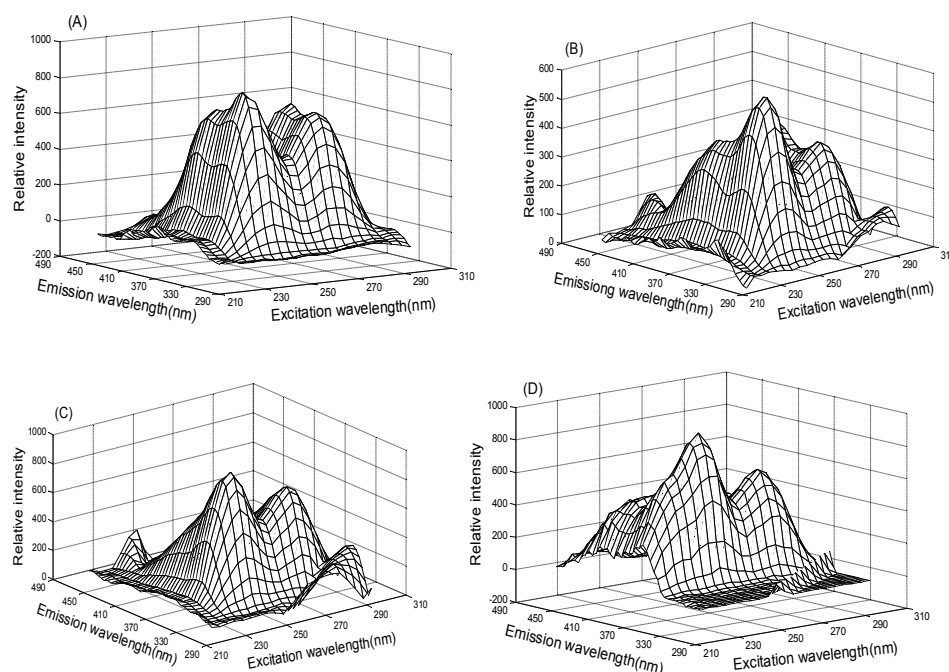


Fig. 5 Three-dimensional plots of the excitation–emission matrix fluorescence spectra: (A) for pure magnolol and honokiol; (B) for Magnoliae Cortex; (C) for Ping-wei tablet and (D) for magnolol and honokiol in plasma.

4.5.1 Simultaneous determination of magnolol and honokiol in Magnoliae Cortex and Ping-wei tablet

By running PARAFAC and SWATLD program with the factor number of three

($N = 3$). The spectra and concentration profiles could be reached, respectively. The SWATLD loadings related to excitation and emission modes were shown in Figure 6A1 and 6B1, respectively. The spectra of pure magnolol and honokiol were obtained by measuring the pure magnolol and honokiol samples and decomposing them by singular value decomposition (SVD). It was also shown in Figure 6A1 and 6B1. We regarded these normalized profiles as the spectra of the pure and used them as reference spectra to evaluate the reliability of the models in the calibration. As could be seen, the loadings of the excitation and emission modes for magnolol and honokiol coincided with the normalized measured excitation and emission spectra for both analytes. The correlation coefficients which calculated the pure spectrum and the ones resolved by SWATLD all exceeded 0.995 for the each individual analyte in this paper. The plus lines represented the loadings for an inherent interference presenting to the trilinear model. Here the interference might be an unknown compound deriving from the Magnoliae Cortex and Ping-wei tablet background or an offset to fit the trilinear model. Similar results were also obtained by using the PARAFAC algorithm. Thus the spectra profiles acquired by PARAFAC were not showed in this article. One could find that the proposed second-order calibration method based on either PARAFAC or SWATLD could yield satisfactory predictive capacity for qualitative analysis of magnolol and honokiol in complex matrices. As could be seen, the degree of overlapping was significant between these two analytes. Under this circumvent, traditional spectra methods might be restricted when they were used for simultaneously analyzing magnolol and honokiol in complex herb matrices, and consequently multi-way algorithm was used to resolve this question.

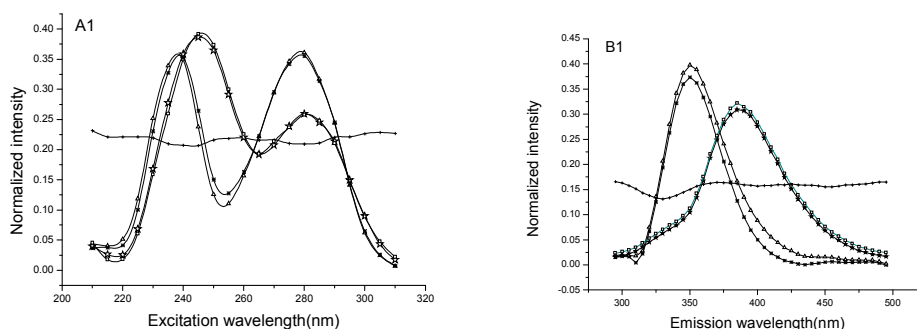


Fig. 6 Normalized EX-EM profiles were resolved by the SWATLD in Magnoliae Cortex and Ping-wei tablet (A1 excitation, B1 emission.). Triangle represented the spectra profiles of pure honokiol, asterisk represent the resolved spectra profiles of honokiol, square brackets represented the spectra profiles of pure magnolol, pentagram represented the resolved spectra profiles of

magnolol, and plus denoted interference.

To further check the accuracy of the PARAFAC and SWATLD method and to study the interference of matrix, analytical recovery experiment was carried out by standard addition method. From the total amount of magnolol and honokiol found, the percentage recovery was calculated. The concentrations of the components in unknown samples were predicted by regressing the loading matrix C (scores) estimated by algorithm on the known concentrations of the calibration samples in the same way as in univariate calibration.

Table 2 Determination results of magnolol and honokiol by EEMs using PARAFAC and SWATLD algorithm in Cortex Magnoliae Officinalis and Ping-Wei tablet ($N = 3$).

	Sample	Magnolol(ug/ml)		Honokiol (ug/ml)		Recovery (%)	
		Actual	Predicted	Actual	Predicted	Magnolol	Honokiol
SWATLD	PM0	-	52.13	-	32.01	-	-
	PM1	35.04	87.94	64.80	89.75	102	89
	PM2	61.32	109.5	50.40	78.03	94	91
	PM3	78.84	126.3	28.89	59.76	94	96
	PP0	-	29.01	-	21.14	-	-
	PP1	43.84	70.86	72.00	89.14	95	94
	PP2	70.08	97.09	57.60	77.87	97	98
	PP3	87.60	111.6	43.20	61.32	94	93
	Average recoveries (%)					96±3	94±3
PARAFAC	PM0	-	52.46	-	32.36	-	-
	PM1	35.04	88.73	64.80	90.16	104	89
	PM2	61.32	109.3	50.40	77.85	92	90
	PM3	78.84	127.4	28.89	59.90	95	95
	PP0	-	29.45	-	21.36	-	-
	PP1	43.84	71.03	72.00	89.33	95	94
	PP2	70.08	96.79	57.60	77.34	96	97
	PP3	87.60	110.9	43.20	62.35	93	95
	Average recoveries (%)					96±3	94±3

Table 2 summarized the results obtained for linear regression method applied to calibration sets for the both analytes. PM1 and PP1 denoted the real sample; PM2-PM4 and PP2-PP4 denoted the standard addition samples with different addition amount of magnolol and honokiol to the diluted extract of Cortex Magnoliae

1
2
3
4
5
6
7
8
9
10
11
12
13
14
15
16
17
18
19
20
21
22
23
24
25
26
27
28
29
30
31
32
33
34
35
36
37
38
39
40
41
42
43
44
45
46
47
48
49
50
51
52
53
54
55
56
57
58
59
60

Officinalis and Ping-Wei tablet in the buffer solution, respectively. The predicted concentration by PARAFAC showed recoveries between 93% and 104% and between 89% and 97% for magnolol and honokiol, respectively. SWALD method showed recoveries between 94% and 102% for magnolol and between 89% and 98% for honokiol. The average recoveries for the PARAFAC procedure were $96\pm 3\%$ for magnolol and $94\pm 3\%$ for honokiol, and SWALD procedure were $96\pm 3\%$ for magnolol and $94\pm 3\%$ for honokiol. The results demonstrated that this method had both high recovery and good precision for magnolol and honokiol. So, in all the cases, recoveries were acceptable for both methods. It showed that the dispersion of the results was lower for SWATLD than that for PARAFAC. On the same time, the iterative numbers of SWATLD were shorter than PARAFAC and insensitive for the chemical rank of the mixture system. This was coincident with the former application [27].

These results proved again that both algorithms could allow for accurate quantitative determination of magnolol and honokiol in complex herb samples, but the SWATLD was specially recommended in the systems suffering from serious matrix effects. In the same time, The determined contents of honokiol and magnolol in Cortex Magnoliae were well in agreement with previous reports (8.0–68.7 mg/g for honokiol and 12.2–96.8 mg/g for magnolol, respectively) [18,21].

4.5.2 Simultaneous determination of magnolol and honokiol in plasma samples

With a similar experimental scheme in the analysis of plasma samples, they included ten calibration (C01-C10) samples and four predicted plasma (PB0-PB3) samples resulting in a cube matrix sized $14_{\text{Sam}} \times 42_{\text{Em}} \times 21_{\text{Ex}}$ (Considering the large datasets might lead to increase the possibility of getting stuck in local minima for iterative algorithm and increase the running time. Here we combined the above mentioned calibration samples and the plasma samples as individual datasets to run multi-way algorithm). Both PARAFAC and SWATLD methods were also utilized to resolve the cube matrix datasets and to quantify magnolol and honokiol in plasma samples with $N = 3$ suggested by the core consistency test and LTMC method. Only The SWATLD loading profiles related to excitation and emission modes together with the actual ones were shown in Figure 7. In Figure 7, the resolved spectral profiles for magnolol and honokiol matched quite well with the true signal of magnolol and honokiol. Obviously, the resolved spectra of magnolol and honokiol were similar to

those obtained from the individual excitation-emission matrix analysis and previously discussed in Section 4.5.1 except that the interference profile in the plasma was different with above analysis samples. Here one could observe that there were heavily overlapped peaks not only between these two analytes but also between the analytes and interference. Under this circumvent, traditional spectra methods could not attain the accurate results of quantitative analysis, and consequently multi-way algorithm was also used to resolve this question. These results further confirmed that the second-order methods in this paper allowed the spectral profiles of analytes of interest to be extract reliably and accurately even in different complex matrices, mainly due to the characteristic of trilinear data. For similar reasons, the spectra profiles acquired by PARAFAC were also not showed in this article.

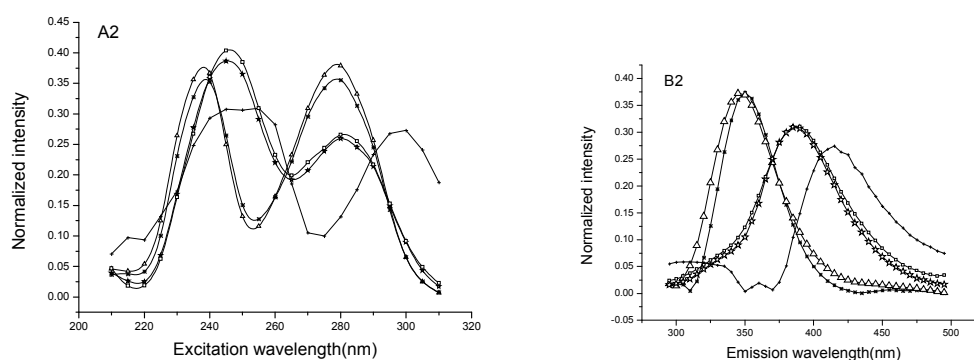


Fig. 7 Normalized EX-EM profiles were resolved by the SWATLD in human plasma (A2 excitation, B2 emission). Triangle represented the spectra profiles of pure honokiol, asterisk represented the resolved spectra profiles of honokiol, square brackets represented the spectra profiles of pure magnolol, pentagram represented the resolved spectra profiles of magnolol, and plus denoted interference.

The scores related to sample mode used for calibration through a linear regression with the prediction results of magnolol and honokiol were shown in Table 3. Because plasma was obtained from healthy volunteers, magnolol and honokiol were not found in real plasma samples. The average recoveries of magnolol in spiked plasma samples using PARAFAC and SWATLD were found to be $102\pm 6\%$ and $102\pm 5\%$, respectively. The average recoveries corresponding to honokiol were $94\pm 1\%$ and $95\pm 2\%$, respectively. This analysis further proved that the multi-way algorithm as a useful and excellent tool for the quantification of analytes of interests in complex samples had exploited the “second-order advantage”.

Table 3 Determination results of magnolol and honokiol by EEMs using PARAFAC and SWATLD algorithm in human plasma ($N = 3$).

Sample	Magnolol ($\mu\text{g/ml}$)		Honokiol ($\mu\text{g/ml}$)		Recovery (%)		
	Actual	Predicted	Actual	Predicted	magnolol	honokiol	
SWATLD	PB0	-	0	-	0	-	-
	PB1	87.60	86.00	108.0	102.3	98	95
	PB2	105.1	104.3	72.00	67.36	104	94
	PB3	70.08	71.80	115.2	110.6	103	96
	Average recoveries (%)					102 \pm 5	95 \pm 2
PARAFAC	PB0	-	0	-	0	-	-
	PB1	87.60	85.47	108.0	110.3	98	94
	PB2	105.1	110.2	72.00	67.90	105	94
	PB3	70.08	72.26	115.2	110.8	103	95
	Average recoveries (%)					102 \pm 6	94 \pm 1

4.6. Method validation

The most important process for comparison of analytical methods is the determination of figures of merit (FOM). To evaluate the performance of the developed method, the validation parameters including sensitivity (SEN), selectivity (SEL), and limit of detection (LOD) have been calculated. In multivariate calibration, the net analyte signal (NAS) calculation [27] is strictly necessary for the FOM evaluation. The NAS for multiway data is analogous to those for first order procedures, which is defined as the part of the signal that relates uniquely to the analyte of interest. In this case, as the data are bilinear, the NAS is the pure analyte data obtained by PARAFAC or SWATLD [25]. The sensitivity is estimated as the NAS at unit concentration, as shown in (7), and the selectivity is the ratio between the sensitivity and the total signal, as shown in (8):

$$\text{SEN} = k \{ [(A^T A)^{-1}]_{nn} [(B^T B)^{-1}]_{nn} \}^{-1/2} \quad (7)$$

$$\text{SEL} = \{ [(A^T A)^{-1}]_{nn} [(B^T B)^{-1}]_{nn} \}^{1/2} \quad (8)$$

Where \mathbf{A} and \mathbf{B} are the matrices which collect excitation and emission spectral profiles for all N components, respectively. n denotes the n th component in mixture system. k denotes the slope of pseudo-univariate plot and represent the total signal for the analyte of interest at unit concentration. The limit of detection (LOD) [36] is calculated as

$$\text{LOD} = 3.3s_{(o)} \quad (9)$$

where $s_{(o)}$ is the standard deviation from the concentration estimated with five different blank samples in the PARAFAC and SWATLD models, respectively. The more details can be found in reference [27].

The SEL, SEN, and LOD values depended strongly on other constituents such as unknown interferences and other analytes of interest in the same spectral region. Table 4 summarized the analytical figures of merit such as sensitivity (SEN), selectivity (SEL) and limit of detection (LOD) in the Cortex Magnoliae Officinalis and Ping-Wei tablet samples. The LOD of magnolol using PARAFAC and SWATLD were found to be 0.51 $\mu\text{g/ml}$ and 0.45 $\mu\text{g/ml}$, and 0.37 $\mu\text{g/ml}$ and 0.24 $\mu\text{g/ml}$ for honokiol, respectively. Chen, etc. have ever used capillary zone electrophoresis to determine magnolol and honokiol in biological fluids [14]. In their research, the LOD of magnolol and honokiol were 1.13 $\mu\text{g/ml}$ and 0.99 $\mu\text{g/ml}$ with a UV detector. When using an LIF detector, the LOD of magnolol and honokiol were 3.20 ng/ml and 4.79 ng/ml , respectively. In our research, the spectra of magnolol and honokiol were not separated with the help of instrument. In the same time, considering the high concentrations of interfering compounds in herb samples, the LOD were yet satisfactory in our research. Between two methods, magnolol showed the lower SEN value. The most important issue was that magnolol had lower selectivity than honokiol. Accordingly, the LOD of magnolol was larger than the one of honokiol. The results from Table 4 including SEL, SEN, and LOD were acceptable.

Table 4 Analytical figure of merit for Cortex Magnoliae Officinalis and Ping-Wei tablet.

Figure of merit ^a	SWALTD		PARAFAC	
	Magnolol	Honokiol	Magnolol	Honokiol
Sensitivity (SEN), ABS, ml/ μg	10.45	5.157	15.92	7.905
Selectivity (SEL)	0.2159	0.2930	0.2275	0.2666
LOD, $\mu\text{g/ml}$	0.45	0.24	0.51	0.37

^aABS is the absorbency intensity (arbitrary units)

Table 5 showed the figures of merit of the proposed method in the human plasma sample. In terms of the figures of merit, honokiol was more selective than magnolol as its spectra were the most different in shape (see Figure 7) from the others and

therefore the least correlated. This preliminary information suggested that honokiol would be predicted at lower concentrations (it is more sensitive). This was confirmed with the LOD calculated. Comparing with the FOM in the Cortex Magnoliae Officinalis and Ping-Wei tablet sample, the LOD value in herb was lower than the one in the human plasma sample. This might be because that the spectra profile of interference was more similarly to the analytes in plasma sample. This led to the selectivity of magnolol decreasing to 0.0812 and 0.0420 in SWATLD and PARAFAC, respectively. In the same time, the sensitivity of magnolol became worse in contrast to them in the Cortex Magnoliae Officinalis and Ping-Wei tablet sample. Even so, the results were yet satisfactory considering the high overlapping of the analytes and high concentrations of interfering compounds in the spectra regions.

Table 5 Analytical figure of merit for human plasma

Figure of merit ^a	SWATLD		PARAFAC	
	Magnolol	Honokiol	Magnolol	Honokiol
Sensitivity (SEN), ABS, ml/μg	68.26	8.217	52.42	16.36
Selectivity (SEL)	0.0812	0.3366	0.0420	0.1474
LOD, μg/ml	0.79	0.42	0.93	0.64

^aABS is the absorbency intensity (arbitrary units)

5. Conclusion

Excitation-emission matrix fluorescence coupling with second-order calibration, in this paper, was used to determine magnolol and honokiol in Cortex Magnoliae Officinalis, Ping-Wei tablet and human plasma. The proposed method avoided preconcentration and with only simple disposal process. The satisfactory recoveries in spiked samples were obtained in all cases when several real samples were analyzed. At the same time, the methodology involving PARAFAC and SWATLD did not require as many calibration samples as the PLS models do and, what is more, enhanced the selectivity and would allow the determination of any of the magnolol and honokiol in the presence of unknown interferences (second-order advantage) even if they were not included in the model. Slightly better results in the complex samples analysis were obtained by application of SWATLD calibration comparing with PARAFAC. This work demonstrated that the use of fluorescence spectroscopy coupling with second-order calibration algorithms was a powerful tool to attain

1
2
3
4
5
6
7
8
9
10
11
12
13
14
15
16
17
18
19
20
21
22
23
24
25
26
27
28
29
30
31
32
33
34
35
36
37
38
39
40
41
42
43
44
45
46
47
48
49
50
51
52
53
54
55
56
57
58
59
60

analytes identification of overlapped constituents for complex analysis of drugs. The figures of merit calculated for both PARAFAC and SWATLD were very similar and the results should be considered satisfactory based on the complexity of the samples analyzed. Extremely important issues such as reduction in the time of analysis and consequently costs and amount of contaminant solvents should also be considered. Thus it can be considered as a green analytical procedure for magnolol and honokiol determination in herb and plasma samples. In the light of these results, the present methodology can be recommended for analysis of the effective constituent in some real applications, such as pharmacokinetic investigations in patients and major pharmacologically active components analysis in herb. Because the instrument involved in the measurement is nonsophisticated, the experiments can be carried out in routine laboratories.

Acknowledgments

The work was financially supported by Foundation of Henan University of Technology (Grant no. 2014JCYJ08).

References

- [1] E. J. Yang, J. Y. Lee, S. H. Park, T. Lee, K. S. Song, *Food and Chemical Toxicology*, 2013, 56, 304-312
- [2] C. C. Shen, C. L. Ni, Y. C. Shen, Y. L. Huang, C. H. Kuo, T. S. Wu, C. C. Chen, *Journal of Natural products*, 2009, 72, 168-171.
- [3] C. Zhao, Z. Q. Liu, *Biochimie*, 2011, 93, 1755-1760
- [4] Z. Li, Y. Liu, X. Zhao, X. Pan, R. Yin, C. Huang, L. J. Chen, Y. Q. Wei, *European Journal of Obstetrics & Gynecology and Reproductive Biology*, 2008, 140, 95-102.
- [5] Y. R. Lin, H. H. Chen, C. H. Ko, M. H. Chan, *Neuropharmacology*, 2005, 49, 542-550.
- [6] M. Alexeev, D. K. Grosenbaugh, D. D. Mott, J. L. Fisher, *Neuropharmacology*, 2012, 62, 2507-2514.
- [7] H. F. Zhai, K. Nakade, Y. Mitsumoto, Y. Fukuyama, *European Journal of Pharmacology*, 2003, 474, 199-204.
- [8] T. H. Kua, Y. J. Leeb, S. J. Wang, C. H. Fan, L. T. Tien, *Phytomedicine*, 2011, 18, 1126-1129.
- [9] S. X. Yu, R. Y. Yan, R. X. Liang, W. Wang, B. Yang, *Fitoterapia*, 2012, 83,

- 356-361.
- [10] J. Park, J. Lee, E. Jung, Y. Park, K. Kim, B. Park, K. Jung, E. Park, J. Kim, D. Park, *European Journal of Pharmacology*, 2004, 496, 189-195
- [11] Editorial Committee of Chinese Materia Medica, *Chinese Materia Medica*, vol. 1, essential ed., Shanghai Science and Technology Press, Shanghai, 1999, pp. 423-432.
- [12] Y. R. Lin, H. H. Chen, C. H. Ko, M. H. Chan, *European Journal of Pharmacology*, 2006, 537, 64-69.
- [13] X. Wu, X. G. Chen, Z. D. Hu, *Talanta*, 2003, 59, 115-121
- [14] C. L. Chen, P. L. Chang, S. S. Lee, F. C. Peng, C. H. Kuo, H. T. Chang, *Journal of Chromatography A*, 2007, 1142, 240-244.
- [15] T. H. Tsai, C.J. Chou, F.C. Cheng, C.F. Chen, *Journal of Chromatography B*, 1994, 655, 41-45.
- [16] T. Nakazawa, T. Yasuda, K. Ohsawa, *Journal of Pharmacological Sciences*, 2003, 55, 1583-1591.
- [17] K. Suto, Y. Ito, K. Sagara, H. Itokawa, *Journal of Chromatography A*, 1997, 786, 366-370.
- [18] P. Aihua, H. Ye, J. Shi, S. He, S. Zhong, S. Li, L. J. Chen, *Journal of Chromatography A*, 2010, 1217, 5935-5939.
- [19] Y. T. Wu, L. C. Lin, T. H. Tsai, *Biomedical Chromatography*, 2006, 20, 1076-1081.
- [20] L. Liu, X. Wu, L. Fan, X. Chen, Z. Hu, *Analytical and Bioanalytical Chemistry*, 2006, 384, 1533-1539.
- [21] G. Chen, X.J. Xua, Y. Z. Zhu, L. Y. Zhang, P. Y. Yang, *Journal of Pharmaceutical and Biomedical Analysis*, 2006, 41, 1479-1484
- [22] J. D. Jiang, H. L. Wu, A L. Xia, S. H. Zhu, D. S. Liu, H. F. Zhang, R. Q. Yu, *Chemical Journal of Chinese Universities*, 2008, 29, 71-76.
- [23] Y. Jun, D. S. Yu, F. S. Liu, Y. F. Tian, B. B. Mo, *Chinese Journal of Analytical Chemistry*, 2009, 37, 107-110
- [24] H. C. Goicoechea, M. J. Culzonia, M. D. G. Garcíab, M. M. Galera, *Talanta*, 2011, 83, 1098-1107.
- [25] K. S. Booksh, B. R. Kowalski, *Analytical Chemistry*, 1994, 66, 782A-791A.
- [26] A. Smilde, R. Bro, P. Geladi, *Multi-Way Analysis with Applications in the Chemical Sciences*; Wiley: Chichester, U.K., 2004, pp. 1-18

- 1
2
3
4 [27] A. C. Olivieri, *Chem. Rev.* 2014, 114, 5358-5378
- 5
6 [28] H. L. Wu, J. F. Nie, Y. J. Yu, R. Q. Yu, *Analytica Chimica Acta*, 2009, 650,
7 131-142.
- 8
9 [29] E. Sanchez, B. R. Kowalski, *Analytical Chemistry*, 1986, 58, 496-499.
- 10
11 [30] R. A. Harshman, *UCLA Working Papers in Phonetics*, 1970, 16, 1-84.
- 12
13 [31] H. L. Wu, M. Shibukawa, K. Oguma, *Journal of Chemometrics*, 1998, 12, 1-26.
- 14
15 [32] J. H. Jiang, H. L. Wu, Z. P. Chen, R. Q. Yu, *Analytical Chemistry*, 1999, 71,
16 4254-4262.
- 17
18 [33] Z. P. Chen, H. L. Wu, R. Q. Yu, *Journal of Chemometrics*, 2001, 15, 439-453.
- 19
20 [34] M. Esteban, C. Arino, J. N. Diaz-Cruz, M. S. Diaz-Cruz, R. Tauler, *Trends in*
21 *Analytical Chemistry*, 2000, 19, 49-61.
- 22
23 [35] A. Espinosa-Mansilla, A. Munoz de la Pena, D. Gonzalez Gomez, F. Salinas,
24 *Analytica Chimica Acta*, 2005, 531, 257-266
- 25
26 [36] R. Bro, H. A. L. Kiers, *Journal of Chemometrics*, 2003, 17, 274-286.
- 27
28 [37] L. Q. Hu, H. L. Wu, J. H. Jiang, Q. J. Han, A. L. Xia, R. Q. Yu, *Talanta*, 2007, 71,
29 373-380.
30
31
32
33
34
35
36
37
38
39
40
41
42
43
44
45
46
47
48
49
50
51
52
53
54
55
56
57
58
59
60